Original Article

http://dx.doi.org/10.3348/kjr.2012.13.6.667
pISSN 1229-6929 · eISSN 2005-8330
Korean J Radiol 2012;13(6):667-673

Korean Journal of Radiology
KJR

# Evaluation of Anterior Ethmoidal Artery by 320-Slice CT Angiography with Comparison to Three-Dimensional Spin Digital Subtraction Angiography: Initial Experiences

Juan Ding, MD[1], Gang Sun, MD, PhD[1], Yang Lu, MD, PhD[2], Bing-bing Yu, MD[1], Min Li, MD[1], Li Li, MD[1], Guo-ying Li, MD[1], Zhao-hui Peng, MD[1], Xu-Ping Zhang, MD[1]

[1]Department of Medical Imaging, Jinan Military General Hospital, Jinan 250031, China; [2]Department of Radiology, University of Illinois College of Medicine, IL 60612, USA

**Objective:** To explore the usefulness of 320-slice CT angiography (CTA) for evaluating the course of the anterior ethmoidal artery (AEA) and its relationship with adjacent structures by using three-dimensional (3D) spin digital subtraction angiography (DSA) as standard reference.

**Materials and Methods:** From December 2008 to December 2010, 32 patients with cerebrovascular disease, who underwent both cranial 3D spin DSA and 320-slice CTA within a 30 day period from each other, were retrospectively reviewed. AEA course in ethmoid was analyzed in DSA and CTA. In addition, adjacent bony landmarks (bony notch in medial orbital wall, anterior ethmoidal canal, and anterior ethmoidal sulcus) were evaluated with CTA using the MPR technique oriented along the axial, coronal and oblique coronal planes in all patients. The dose length product (DLP) for CTA and the dose-area product (DAP) for 3D spin DSA were recorded. Effective dose (ED) was calculated.

**Results:** The entire course of the AEA was seen in all 32 cases (100%) with 3D spine DSA and in 29 of 32 cases (90.1%) with 320-slice CTA, with no significant difference ($p = 0.24$). In three cases where AEA was not visualized on 320-slice CTA, two were due to the dominant posterior ethmoidal artery, while the remaining case was due to diminutive AEA. On MPR images of 320-slice CT, a bony notch in the orbital medial walls was detected in all cases (100%, 64 of 64); anterior ethmoidal canal was seen in 28 of 64 cases (43.8%), and the anterior ethmoidal sulcus was seen in 63 of 64 cases (98.4%). The mean effective dose in CTA was 0.6 ± 0.25 mSv, which was significantly lower than for 3D spin DSA (1.3 ± 0.01 mSv) ($p < 0.001$).

**Conclusion:** 320-slice CTA has a similar detection rate for AEA to that of 3D spin DSA; however, it is noninvasive, and may be preferentially used for the evaluation of AEA and its adjacent bony variations and pathologic changes in preoperative patients with paranasal sinus diseases.

**Index terms:** *Computed tomography angiography; 320-slice CT; Anterior ethmoid artery; Digital subtraction angiography*

Received May 15, 2011; accepted after revision April 3, 2012.
**Corresponding author:** Gang Sun, MD, PhD, Department of Medical Imaging, Jinan Military General Hospital, 25 Shifan Road, Jinan 250031, China.
• Tel: (86531) 51666864 • Fax: (86531) 51666864
• E-mail: cjrsungang@163.com


## INTRODUCTION

The anterior ethmoid artery (AEA) running through the roof of anterior ethmoid sinuses as it traverses from the orbit to the anterior cranial fossa, is a major anatomical landmark that is vulnerable to accidental injury during surgery on the anterior ethmoidal sinus. Its injury may result in profuse epistaxis, intraorbital bleeding and retro-orbital hematoma that can lead to blindness (if not decompressed

within approximately an hour), and cerebrospinal fluid leak or in rare cases, intracranial bleeding (1).

Due to the wide variation in the localization, course, and length of the AEA, it is important to have an accurate preoperative evaluation of AEA. Three-dimensional (3D) spin digital subtraction angiography (DSA) is a 3D acquisition mode which can provide a superior spatial and temporal resolution for AEA assessment, and considered the gold standard. However, this technique is an invasive procedure that requires the placement of a catheter in the carotid artery through the femoral artery. Contrast dye is then injected directly into the carotid artery, and X-rays are taken to record the course of AEA. This invasive nature and potential risks for microembolic events in patients with cerebral vascular disease limits its widespread use (2, 3). Therefore it would be desirable to replace DSA with non-invasive studies.

With the development of computed tomography (CT) scanning techniques, the comprehensive, noninvasive assessment of the anatomy and possible lesions in cranial vascular structures using computed tomographic angiography (CTA) has become possible (4). Many studies worldwide have provided some guidelines to improve the identification and localization of the artery during surgery (5-9). However, a major limitation of the CT exam for AEA was only demonstrated on adjacent bony landmarks, and was clinically difficult to locate the artery purely based on these data; particularly due to the anatomical variations and pathological status of the paranasal sinus.

The volume CT technique introduced in the novel 320-slice CT scanner enables noninvasive angiographic imaging of the entire cranial vasculature in a single rotation, which could maintain satisfactory spatial resolution with a desired temporal resolution (10, 11).

To explore the usage of the 320-slice CT scanner for evaluation of AEA course and its relationship with adjacent structures, we utilized CTA combined with multiplanar reformations (MPR) and maximum intensity projection (MIP) methods in 32 patients with cerebral vascular and tumor disease. The obtained images were compared with MIP images acquired from the 3D spin DSA technique in the same patient, with the latter as the standard of reference.

## MATERIALS AND METHODS

### Patients

From December 2008 and March 2010, a total of 32 patients in our hospital had both CT and DSA within 30 day intervals. Prior informed consent was obtained from all patients. Information from patient medical records and radiographic studies were retrospectively reviewed with the approval of our Institutional Review Board. These patients were affected by intracranial aneurysms (30 cases), and meningioma (2 cases). The subjects comprised 25 males and 7 females ranging in age from 25 to 75 years old (means 47.2 years). All patients had no history of surgery or trauma in paranasal sinuses or the skull base, congenital anomalies of the face, paranasal sinuse malignancies, and ostefibrous lesion.

### Image Acquisition

All CT examinations were performed using the Aquilion ONE multidetector row CT scanner (Toshiba, Medical Systems, Tokyo, Japan) equipped with 320 x 0.5 mm detector rows allowing for a 160 mm scan width during a single rotation.

The CTA data acquisition was performed according to an established protocol of the volume mode. The parameters included an 80 kV tube voltage and 150 effective mAs, 0.75 second rotation time, section thickness of 0.5 mm, a field of view (FOV) of 180 $mm^2$ and 16 cm scanning length covering the entire cranium and orbital with only one single rotation in the artery phrase.

For all examinations, an additional unenhanced volume CT (parameters were the same as that of CTA images) was routinely performed to identify bony structures that were subsequently masked on CTA images. Vessel enhancement was then achieved by intravenously injecting 60-mL contrast material (Ultavist 370; Bayer Schering Pharma, Berlin, Germany), followed by a 40-mL saline flush through an 18-gauge catheter. Flow rate was kept constant at 5 mL/sec throughout the procedure. CT scanning was started manually at the arterial phase, as soon as the operator identified the arrival of the injected contrast medium at the basilar artery trunk by using a bolus tracking technique (SureStart Protocol, Toshiba Medical Systems, Tokyo, Japan).

Raw data were reconstructed on the console or by using dedicated workstation software (Vitrea fX version 1.0; Vital images, Inc., Minnetonka, MN, USA). The vascular information or other anatomical structures could be visualized using the CTA software (including subtraction and volumes for mask in which bony structure can be removed automatically). AEA and adjacent bony landmarks were

Korean Journal of Radiology
KJR

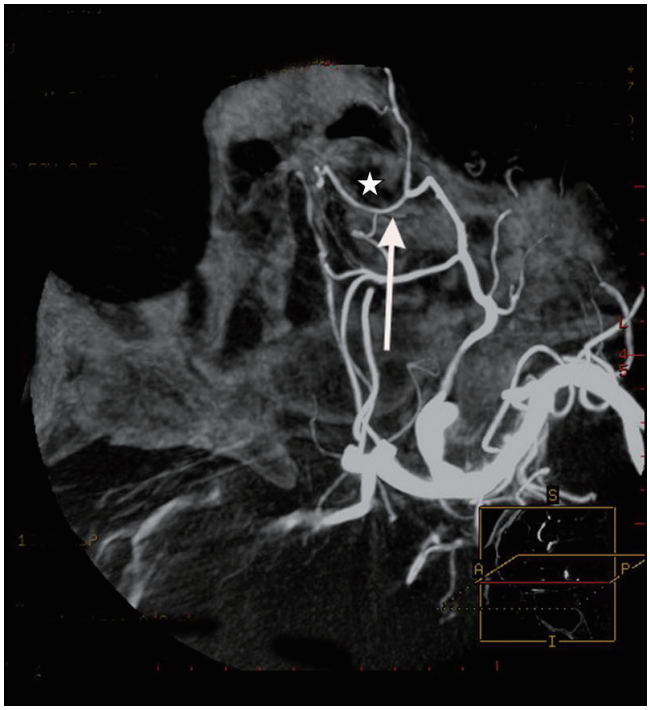

**Fig. 1. Axial maximum intensity projection image of three-dimensional spin digital subtraction angiography shows anterior ethmoid artery over its entire course (arrow) along with its relationship with ethmoidal cells (asterisk).**

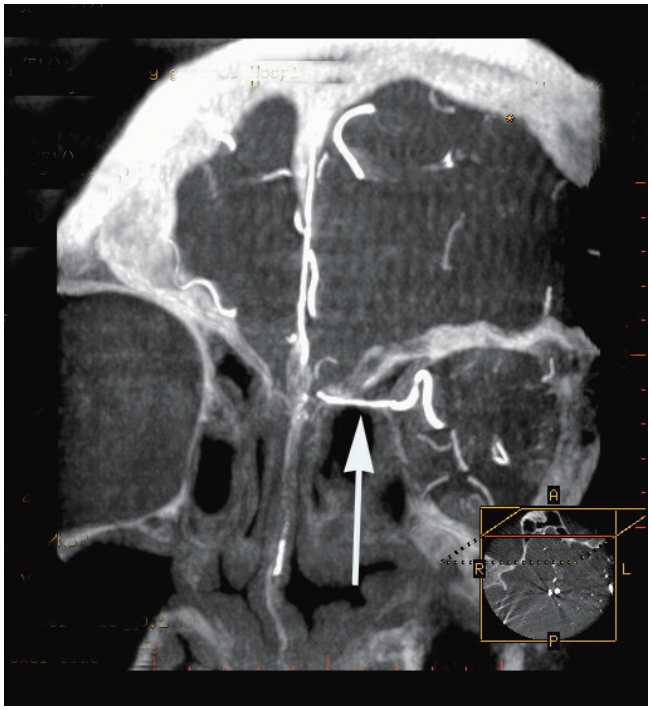

**Fig. 2. Same patient with Fig. 1.** Coronal maximum intensity projection image of three-dimensional spin digital subtraction angiography well depicts intra-ethmoidal course of anterior ethmoid artery (arrow).

evaluated by means of MIP, volume rendering, and MPR technique oriented along the axial, coronal planes and with oblique coronal reconstruction in all patients, respectively.

Invasive selective internal carotid angiography was performed using a transfemoral approach with a C-arm digitalized X-ray system (Innova 4100, GE, Waukesha, WI, USA). The angiography images were acquired with a FOV extended to the ethmoidal region. MIP images with Innova CT reformation software (GE, Waukesha, WI, USA) were generated during an ordinary angiography procedure. MIP images data from a spin angiography (automatic adaptation of kV, mA and time of exposure, FOV 20 cm) which run at a C-arm angle of 240° were reconstructed on the Advantage workstation (Innova 3D XR 1.0 GE, Waukesha, WI, USA) in approximately 7 seconds.

### Image Analysis/Interpretation

The AEA evaluation was performed unilaterally and bilaterally by DSA and CTA, respectively. AEA course in ethmoid was analyzed by DSA and CTA. In addition, adjacent bony landmarks (bony notch in the medial orbital wall, anterior ethmoidal canal and anterior ethmoidal sulcus) were evaluated in CTA by means of the MPR technique oriented along the axial, coronal and oblique coronal planes in all patients. All observations were performed independently by two readers and the results were evaluated by consensus.

### Radiation Exposure

The dose length product (DLP) for CTA (including the unenhanced CT and CTA scans) and the dose-area product (DAP) for 3D spin DSA were recorded. Effective dose (ED) was calculated by using the International Commission on Radiological Protection's conversion factor for cranial CT (0.0021) (12).

### Statistical Methods

Statistical analyses were performed with SPSS version 16 for Windows (SPSS Inc., Chicago, IL, USA). A $p$ value of less than 0.05 was set as the threshold for statistical significance. The detection rate of AEA on the same side with CTA and DSA were compared using Fisher's exact test. Identification rate of the bony notch in the medial wall of the orbit, the anterior ethmoidal canal, and the anterior ethmoidal sulcus were recorded in CTA by means of MPR. a paired $t$ test was performed to evaluate the radiation exposure between CTA and 3D spin DSA. The interobserver agreement was calculated using kappa statistics. Kappa

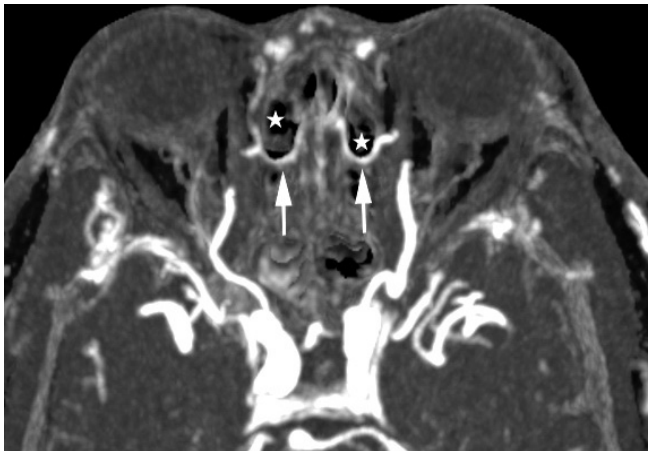

**Fig. 3. Axial maximum intensity projection image of computed tomographic angiography shows entire course of bilateral anterior ethmoid arterys (arrows) and their relationship with ethmoidal cell (asterisks) in patient with meningioma.**

**Fig. 6. Axial multiplanar reformations image shows bony notch (arrowhead) on medial wall of orbits, corresponding to anterior ethmoidal foramen.**

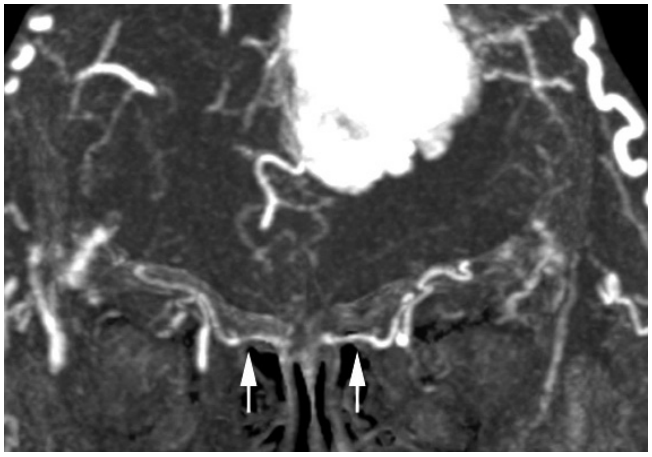

**Fig. 4. Same patient with Fig. 3.** Coronal maximum intensity projection image of computed tomographic angiography well depicts intra-ethmoidal course of bilateral anterior ethmoid arterys (arrows).

**Fig. 7. Coronal multiplanar reformations image shows anterior ethmoidal canal (arrows) through anterior ethmoidal cells, which corresponds to anterior ethmoid artery in its ethmoidal route.**

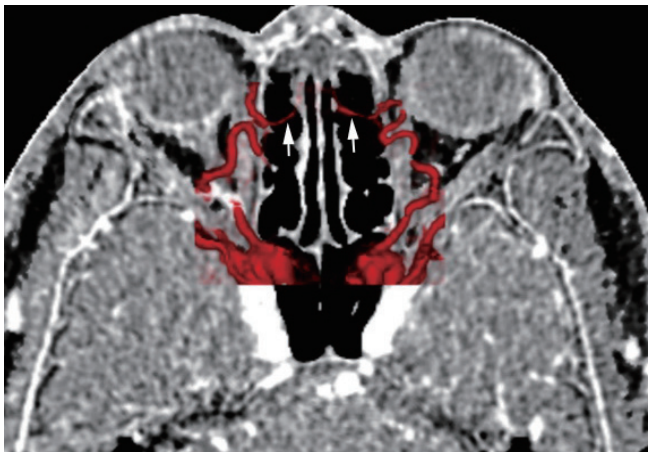

**Fig. 5. Volume rendering overlapping multiplanar reformations image of computed tomographic angiography shows bilateral anterior ethmoid arterys (arrows) and their crossed adjacent anatomical structures.**

**Fig. 8. Coronal multiplanar reformations image shows anterior ethmoidal sulcus-bony sulcus (arrows) on lateral walls of olfactory fossae, corresponding to anterior ethmoidal sulci.**

Korean Journal of Radiology
KJR

values less than 0.20 were interpreted as poor agreement, 0.21-0.40 as fair agreement, 0.41-0.60 as moderate, 0.61-0.80 as good and 0.81-1.00 as very good agreement (13).

## RESULTS

The entire AEA course in the ethmoid was seen in all cases (100%, 32/32) on images of 3D spin DSA, among which 29 of 32 cases (90.1%) on the corresponding side with 3D spin DSA were found in CTA. There was no significant difference ($p$ = 0.24) in the detection of AEA between images of 3D spin DSA and CTA. In 3 cases which AEA was not shown by means of CTA, dominant posterior ethmoidal artery was seen in 2 cases with diminutive AEA, while simple diminutive AEA was seen in the rest. In the displayed unilateral AEA, its entire course was characterized on the axial plane in the form of a curve with concavity in images of 3D spin DSA and CTA (Figs. 1-4). Bilateral AEAs and the adjacent anatomical structures could be assessed on images of CTA based on the use of the VR (Fig. 5), MIP and MPR techniques. However, only unilateral AEA could be visualized on images of 3D spin DSA. The entire AEA course in the ethmoid was seen in the bilateral position in 59 of 64 cases (92.2%) on CTA images. Results of AEA with two methods were exactly the same between the two readers. The interobserver agreement was excellent (k = 0.833).

In assessing the anatomical landmarks for locating AEA by means of MPR in axial and coronal CT images, the bilateral bony notch in the orbital medial wall was detected in all 64 cases (100%) (Fig. 6), whereas the bilateral anterior ethmoidal canal was seen in 28 of 64 cases (43.75%) (Fig. 7), and the bilateral anterior ethmoidal sulcus was seen in 63 of 64 cases (98.44%) (Fig. 8). The interobserver agreement was calculated as k = 0.782, which corresponds to good agreement.

The dose-length product (DLP) for CTA was 265.63 ± 11.30 mGy·cm, and the DAP was 620.46 ± 5.72 mGy·cm$^2$) for DSA. The ED was 0.56 ± 0.25 and 1.32 ± 0.01 mSv for CTA and DSA, respectively (Table 1). A significant difference in ED was found between CTA and 3D spin DSA ($p$ < 0.001).

## DISCUSSION

The AEA is an important anatomical landmark in the surgical approach to the frontal recess and anterior skull base (14, 15). Overall, the AEA crosses three cavities: the orbital, the ethmoidal labyrinth, and the anterior cranial fossa. It arises from the distal ophthalmic artery in the orbital cavity, extends medially, and crosses the anterior ethmoidal foramen (the bony notch on the medial wall of the orbits) into the anterior ethmoid. In its ethmoidal route, the AEA lies inside the anterior ethmoidal canal or ethmoidal lamella. The AEA runs through the ethmoidal ceiling posterior-inferiorly in a diagonal direction, and then through the anterior ethmoidal sulcus it penetrates into the skull lining between the cribiform plate and the olfactory cleft lateral lamella (16).

In the ethmoid area, AEA is at high risk for incidental injury during surgery due to its deep location, variable position relative to the ethmoidal roof, and complicated connections with adjacent structures. Damage to the artery may cause serious complications, such as intense intraorbital bleeding or orbital hematoma that may cause blindness within 1 hour without effective treatment, cerebrospinal fluid leak, and even meningitis and cerebral infections. Thus, it is extremely important for the preoperative evaluation of AEA (1).

Though DSA is regarded as the "gold standard", with its superior imaging quality for the evaluation of AEAs, its invasive nature limits its clinical application, especially in patients with benign rhinosinus. Here, we applied 3D DSA as the standard to validate data from a 320-slice CTA.

Indirect identification of AEA through anatomical bony landmarks has been widely applied at the clinical level. To this point, the CT technique is advantageous compared to DSA. For all 32 patients, the bilateral medial notch of the orbit were shown in all 64 cases (100%), while the anterior ethmoidal sulcus was shown in 63 of 64 cases 98.44%, and the anterior ethmoidal canals were shown in 28 of 64 cases (43.75%), respectively on MPR images, which was in keeping with published data from other groups. Souza et al. (6) retrospectively reviewed 198 coronal paranasal sinus

**Table 1. Radiation Exposure Dose for CTA and 3D Spin DSA**

| Parameters | DLP (mGy·cm) | DAP (mGy·cm$^2$) | Effective Dose (mSv) |
|---|---|---|---|
| CTA | 265.63 ± 11.30 | | 0.56 ± 0.25 |
| 3D spin DSA | | 620 ± 5.71 | 1.3 ± 0.01 |

**Note.**— DLP = dose length product, DAP = dose-area product, ED = effective dose, CTA = computed tomography angiography, DSA = digital subtraction angiography

CT exams with 3 mm contiguous slices, and found that the medial notch of the orbit, anterior ethmoidal sulcus, and anterior ethmoidal canal were seen in all 198 cases, 194 of 198 cases (98%), and 81 of 198 cases (41%), respectively. Başak et al. (7) identified the anterior ethmoidal canal in 43% of cases that underwent a coronal plane CT. Pandolfo et al. (8) analyzed AEAs in 20 patients with cerebrovascular disease, and another 78 patients with inflammatory disease and polyposis by a 16-slice multislice CT scanner with a 0.7 mm thickness. They also reported the indirect detection of AEA through the visualization of the entry point of the vessel in the ethmoid or the medial notch of the orbit, in all cases n = 20 (100%) on MPR images.

Though the essential relations between AEA and orbit, anterior cranial fossa, and sphenoid, were always analyzed in most published papers, the course of AEA was not reported. Furthermore, there has been no well-analyzed AEA data from cases using the CTA technique. The recently developed novel 320-slice CT scanner can cover 16 cm in the z-axis, which enables coverage of the entire head in a single rotation. Different from the helical scan mode in previous multi-slice CT (8 or 16 or 64), volume scan mode was adopted in the 320-slice CT. The disadvantage of the step artifact when using a helical scan could be avoided without the movement of patients and the bed during examination. Moreover, the cranial vasculature including AEA could be clearly visualized because the adjacent bony structures were more thoroughly removed more.

Aquilion ONE 320-slice CT scanner has been applied ever since December 2008 in our hospital. In this retrospective review, we analyzed patients who underwent both cranial CTA and DSA within 1 month intervals for the two techniques in our hospital. A total of 32 patients were included in this study. Though CTA capable of visualizing bilateral AEAs, comparisons were performed on the unilateral AEAs corresponding to the DSA, which served as standard references. There was no significant difference ($p$ = 0.24) in the identification of the AEA course between DSA (100%, 32 of 32 cases) and CTA (90.6%, 29 of 32 cases). In 3 cases where AEA was not shown by means of CTA, the dominant posterior ethmoidal artery was seen in 2 cases with diminutive AEAs, while simple diminutive AEA was seen in the remaining cases. The reason for this is that the density of contrast-enhanced is so high, that AEA could not be distinguished from the adjacent bone. In this retrospective study, all patients had a normal paranasal sinus condition, while the majority of the patients who underwent paranasal sinus surgery have paranasal sinus diseases. AEA is usually encircled by pathologic tissue with effacement of bony lamella, in most cases with inflammatory disease and polyposis. Assumedly the bone would be easier to differentiate from AEA during the pathological status, it could be expected that AEA in the ethmoidal should be detected at a much higher rate than that in non-pathologic conditions.

All the CTA were obtained using a cranial scan protocol rather than the specific protocol for AEA, which resulted in a larger scan scope. The mean ED including unenhanced CT and CTA in the 320-slice CT studies was 0.56 ± 0.25 mSv, which was significantly lower than that of the 3D spin DSA (1.32 ± 0.01 mSv). When the dedicated AEA scan with a rather narrow scan scope is defined by the anatomical structures on which it was performed, ED should be further reduced. In addition, CTA may demonstrate bilateral AEA and its adjacent boney landmarks. In this group, the entire AEA course in the ethmoid bilaterally was seen in 59 cases (92.2%, 59 of 64 cases) by CTA.

The limitations of the present study are as follows: first, the AEA detection of CTA is known to be influenced by paranasal sinus diseases. However, enrolled patients have normal paranasal sinuses, which may result in an inaccurate evaluation of the AEA. Second, specific scan protocol for AEA was not applied in the study, which should remarkably decrease the radiation dose.

In conclusion, to ensure the safety and efficiency of paranasal sinus surgery, it is essential for preoperative evaluation of the course of AEA. Our results showed that CTA using the 320-slice CT scanner was a 3D-DSA comparison, while the noninvasive imaging modality for visualization of AEA course in lower radiation dose, is the inherent advantage of directly identifying AEA and visualization of adjacent bony anatomical landmarks. Lastly, CTA may work better in the evaluation of AEA in patients with bony variations of paranasal sinuses, and/or other paranasal sinus diseases with ethmoidal bony construction effaced by pathologic tissues, assuming the bone would be easier to differentiate from AEA during pathological status.

## REFERENCES

1. Simmen D, Raghavan U, Briner HR, Manestar M, Schuknecht B, Groscurth P, et al. The surgeon's view of the anterior ethmoid artery. *Clin Otolaryngol* 2006;31:187-191
2. Willinsky RA, Taylor SM, TerBrugge K, Farb RI, Tomlinson G, Montanera W. Neurologic complications of cerebral

angiography: prospective analysis of 2,899 procedures and review of the literature. *Radiology* 2003;227:522-528
3. Leffers AM, Wagner A. Neurologic complications of cerebral angiography. A retrospective study of complication rate and patient risk factors. *Acta Radiol* 2000;41:204-210
4. Klingebiel R, Busch M, Bohner G, Zimmer C, Hoffmann O, Masuhr F. Multi-slice CT angiography in the evaluation of patients with acute cerebrovascular disease--a promising new diagnostic tool. *J Neurol* 2002;249:43-49
5. Cankal F, Apaydin N, Acar HI, Elhan A, Tekdemir I, Yurdakul M, et al. Evaluation of the anterior and posterior ethmoidal canal by computed tomography. *Clin Radiol* 2004;59:1034-1040
6. Souza SA, Souza MM, Gregório LC, Ajzen S. Anterior ethmoidal artery evaluation on coronal CT scans. *Braz J Otorhinolaryngol* 2009;75:101-106
7. Başak S, Karaman CZ, Akdilli A, Mutlu C, Odabaşi O, Erpek G. Evaluation of some important anatomical variations and dangerous areas of the paranasal sinuses by CT for safer endonasal surgery. *Rhinology* 1998;36:162-167
8. Pandolfo I, Vinci S, Salamone I, Granata F, Mazziotti S. Evaluation of the anterior ethmoidal artery by 3D dual volume rotational digital subtraction angiography and native multidetector CT with multiplanar reformations. Initial findings. *Eur Radiol* 2007;17:1584-1590
9. Gotwald TF, Menzler A, Beauchamp NJ, zur Nedden D, Zinreich SJ. Paranasal and orbital anatomy revisited: identification of the ethmoid arteries on coronal CT scans. *Crit Rev Comput Tomogr* 2003;44:263-278
10. Salomon EJ, Barfett J, Willems PW, Geibprasert S, Bacigaluppi S, Krings T. Dynamic CT angiography and CT perfusion employing a 320-detector row CT: protocol and current clinical applications. *Klin Neuroradiol* 2009;19:187-196
11. Klingebiel R, Siebert E, Diekmann S, Wiener E, Masuhr F, Wagner M, et al. 4-D Imaging in cerebrovascular disorders by using 320-slice CT: feasibility and preliminary clinical experience. *Acad Radiol* 2009;16:123-129
12. Christner JA, Kofler JM, McCollough CH. Estimating effective dose for CT using dose-length product compared with using organ doses: consequences of adopting International Commission on Radiological Protection publication 103 or dual-energy scanning. *AJR Am J Roentgenol* 2010;194:881-889
13. Zhang JJ, Liu T, Feng Y, Wu WF, Mou CY, Zhai LH. Diagnostic value of 64-slice dual-source CT coronary angiography in patients with atrial fibrillation: comparison with invasive coronary angiography. *Korean J Radiol* 2011;12:416-423
14. Akdemir G, Tekdemir I, Altin L. Transethmoidal approach to the optic canal: surgical and radiological microanatomy. *Surg Neurol* 2004;62:268-274; discussion 274
15. Abuzayed B, Tanriover N, Gazioglu N, Sanus GZ, Ozlen F, Biceroglu H, et al. Endoscopic endonasal anatomy and approaches to the anterior skull base: a neurosurgeon's viewpoint. *J Craniofac Surg* 2010;21:529-537
16. White DV, Sincoff EH, Abdulrauf SI. Anterior ethmoidal artery: microsurgical anatomy and technical considerations. *Neurosurgery* 2005;56(2 Suppl):406-410; discussion 406-410